NJC

Accepted Manuscript

This is an *Accepted Manuscript*, which has been through the Royal Society of Chemistry peer review process and has been accepted for publication.

Accepted Manuscripts are published online shortly after acceptance, before technical editing, formatting and proof reading. Using this free service, authors can make their results available to the community, in citable form, before we publish the edited article. We will replace this *Accepted Manuscript* with the edited and formatted *Advance Article* as soon as it is available.

You can find more information about *Accepted Manuscripts* in the Information for Authors.

Please note that technical editing may introduce minor changes to the text and/or graphics, which may alter content. The journal's standard Terms & Conditions and the Ethical guidelines still apply. In no event shall the Royal Society of Chemistry be held responsible for any errors or omissions in this *Accepted Manuscript* or any consequences arising from the use of any information it contains.

ROYAL SOCIETY OF CHEMISTRY

www.rsc.org/njc

TOC

Text:

Ancillary ligand substitution proves to be an effective way to produce the blue shift of electroluminescence peak wavelength.

Graphic:

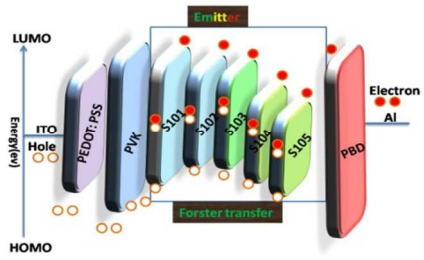

Cite this: DOI: 10.1039/c0xx00000x

www.rsc.org/xxxxxx

ARTICLE TYPE

Key Role of Ancillary Ligand in Imparting Blue Shift in Electroluminescence Wavelength in Ruthenium Polypyridyl Light-Emitting Diodes

HashemShahroosvand[a]*, Shiva Rezaei[a],EzeddinMohajerani[b], MalekMahmoudi[b], Mohammad Ali Kamyabi[a], ShohrehNasiri[a]

[a]Chemistry Department, University of Zanjan, Zanjan, Iran.

[b]Laser and Plasma Research Institute, Shahid Beheshti University, Tehran, Iran.

Received (in XXX, XXX) XthXXXXXXXXX 20XX, Accepted Xth XXXXXXXXX 20XX

DOI: 10.1039/b000000x

The synthesis; characterization and electrochemical, photoluminescence and electroluminescence properties of new ruthenium(II) polypyridyl complexes bearing dpq(COOH)$_2$ ligand, [(phen/or bpy)$_n$Ru(L)$_{3-n}$]$^{2+}$ (n = 0,1,2), where bpy=2,2-bipyridine, phen=1,10-phenanthroline and L=6,7-dicarboxylicdipyrido[2,2-*d*:2',3'*f*] quinoxaline(dpq(COOH)$_2$), (coded as S101-105, respectively), is presented. The five complexes differ in the number and type of the ancillary groups, which are either bpy or phen. Cyclic voltammetry of S101-105 exhibited a reversible one-electron oxidation wave and four one-electron reduction waves. The electroluminescence wavelengths of the complexes (S101-S105) were varied using different ancillary ligands from 485 to 572 nm, respectively. The role of ancillary ligands in the electroluminescence devices of Ru(dpq(COOH)$_2$) complexes was investigated by comprehensive DFT and TD-DFT approaches which indicated that the lowest unoccupied molecular orbital (LUMO) of S101-105 is localized on the distal portion of the dpq(COOH)$_2$ ligand and the highest occupied molecular orbital (HOMO) in the donor region. The highest luminance of 1357 (cd m^{-2}) and lowest turn on of 6.4 (V) were observed in light emitting diodes based on S101 containing 2 equivalents of bpy as ancillary ligands and 1 equivalent of dpq(COOH)$_2$, which is comparable to the maximum electroluminescence properties for Ru polypyridyl emitters. These values represent a new class in the field of organic light emitting diodes using less expensive Ru(II) polypyridyl complexes. The number of carboxylic moiety substituent in these complexes played a significant role in lowering the tendency to aggregate and presenting a better electroluminescence efficiency than that of complexes derived from the phen ligand in a device. As an important result, the incorporation of bpy as ancillary ligand to [Ru(dpq(COOH)$_2$] was found to be the most beneficial ancillary substitution in terms of decreasing the electroluminescence wavelength. These observations suggest that an ancillary ligand can be used to actively control the electroluminescence wavelength by means of tuning the energy level.

1. Introduction:

Ruthenium (II) polypyridyl complexes have received much interest because of their extensive applications in the field of photochemistry, photophysics, and biochemistry [1]. These investigations have mainly focused on the synthesis and construction of new ligands and their corresponding ruthenium polypyridyl complexes capable of performing useful energy conversion and light induced functions [2]. The strong absorbance caused by metal to ligand charge transfer (MLCT), their luminescent characteristics and their reversible redox states provide practicable means to explore their luminescence properties [3]. Furthermore, high-brightness and high-efficiency emissions with a low-driving voltage make them attractive as luminophores for chemi-and electroluminescent devices [4]. Moreover, the electroluminescence color tuning to achieve blue, green, and red is very vital because mixing these colors can produce white, which is crucial for full color display applications [5].The electroluminescence color of ruthenium(II) polypyridyl complexes can be controlled through four dimensions: first, *the ancillary ligand of ruthenium(II) polypyridyl complexes* plays a key role in the spectral properties and the tuning of electroluminescence color. For example, the insertion of 4′-carboxylic ethyl ester in 2,2′,6′,2″, terpyridine in [Ru(tpy)(tpy-COOEt)] /PF_6^- [6] complex leads to an EL spectrum with maxima at 706 nm, whereas [Ru(tpy)$_2$] $^{2+}$ without any anchoring group shows an EL emission in 660 nm [7]. Secondly, *adding groups to the periphery of the ruthenium polypyridyl complexes* further expands the functionality of these complexes. For example, insertion of 4,4′-biphenyl (dp) segments in a 2,2′-bipyridyl(bpy) ligand in the complex Ru(dp-bpy)$_3^{2+}$ enables the tuning of the EL wavelength from 608 to 635 nm [8], whereas insertion of 4,7-dimethyl-1,10-phenanthroline group in the complex Ru(dmphen)$_3^{2+}$ / $C_2O_4^{2-}$ shifts the wavelength of EL spectrum to 590 nm [9] (please see ESI, S1 for more samples). Thirdly, the approach can be performed by using *the mixed ligand substitution in ruthenium polypyridyl complexes.* For example the presence of both 2-(2-pyridyl)-1H-benzoimidazole (PBIm-H) and 2,3-bis(2-pyridyl)benzoquinoxaline (pbq) in [(PBIm-H)$_2$Ru(pbq)]$^{2+}$ complex, shifts the EL spectra to near IR region (940 nm) [10].

Finally, *hetronuclear ruthenium polypyridyl complexes* have been reported as a new emitter class in LED fields. For example, di-nuclear complex of $[Ru(PBIm\text{-}H)_2]_2(pbq)^{+2}$ indicated the maxima EL spectrum at 1040 nm [10]. The π-conjugated chelating ligands in the above examples are one key point to improve the luminescence properties of ruthenium polypyridyl complexes. In addition, π -electron conjugation over the aromatic parts allows a long-distance, yet sufficiently strong electronic interaction between those units [5b]. Dipyrido[3,2-f:2,3-h]-quinoxaline (dpq) as a derivative of 1,10-phenanthroline is an excellent chelating ligand and possesses an extensive p-conjugated system, so it is a good candidate for the construction of electroluminescent complexes . Also, among a great number of bridging ligands containing groups, dicnq derivates as rigid π-conjugated systems are ideal because they prevent bending along and/or rotation around the σ-skeleton of the molecule [11]. In recent years, many researchers have turned their attention to ruthenium complexes containing dpq, which is structurally related to but less conjugated than dppz [12]. Meanwhile, Ambroise et al. reported that $[Ru(phen)(dicnq)_2]^{2+}$ and $[Ru(phen)_2(dicnq)]^{2+}$ {dicnq = 6,7-dicyanodipyrido[2,2-d:2′,3′-*f*]quinoxaline} acted as DNA molecular light switches with emission intensity enhancement factors of 8 and 16, respectively [13]. Kelly and Kruger reported that the incorporation of an amide group to dpq caused a major effect on the excited-state properties of its Ru(II) complex of $[Ru(phen)_2dpqa]^{2+}$ {dpqa = 2-pentylamidodipyrido-[3,2-f:2′,3′-*h*]-quinoxaline}, which did not emit in water but exhibited strong luminescence in DNA environment, thus acting as a good DNA molecular light-switch [14]. However, the electroluminescence studies based on dpq have yet to be reported. With our ongoing interest in electroluminescent ruthenium(II) polypyridyl complexes as the emitter layer in OLED [15], we envisage that ruthenium(II) polypyridyl complexes containing a π-extended ligand have a high potential to serve as new electroluminescent emitters for light emitting diodes. Previously, we have studied the LED properties of ruthenium(II) polypyridyl-based tetrazole derivates [16]. Based on these results, it is of interest to examine ligands that contain both π-extended aromatic rings and functional groups substituted on the two positions of dpq.

In this work, we have synthesized a new interesting class of Ru(II) complex of $\{Ru[(dpq)(COOH)_2)]_x\ (L)_{3-x}\}^{2+}$ (L=bpy, phen) with two carboxylic groups being grafted to the pyrazine ring of dpq. These new materials serve as suitable emitters for a range of distinctive green to blue emitters possessing wide structural features, giving EL devices with tunable color.

2. Experimental:

2.1 Materials and Methods

All chemicals and solvents were purchased from Merck & Aldrich and used without further purification. IR spectra were recorded on a Perkin-Elmer 597 spectrometer. ^{1}H-NMR spectra were recorded using a Bruker 250 MHz, spectrometer. Electrochemical studies (in MeCN) were performed with a μAutolab PGSTAT 101 electrochemistry system. In cyclicvoltammetry (CV) the following parameters and relation were used: scan rate, 100 mV s^{-1}; formal potential $E^{o'} = (E_{pa} + E_{pc}) / 2$ where E_{pa} and E_{pc} are anodic and cathodic peak potentials, respectively; ΔE_p is the peak-to-peak separation. All experiments were done under a dry N_2 atmosphere at 25 °C in a three-electrode configuration by using a Pt-disk working electrode and a Pt-wire auxiliary electrode. The potentials are referenced to a saturated Ag/AgCl reference electrode. The oxidation (E_{ox}) and reduction (E_{red}) potentials were used to determine the HOMO and LUMO energy levels using the equations E_{HOMO} =- (E_{ox} + 4.8) eV and E_{LUMO} = -(E_{red} + 4.8) eV which were calculated using the internal standard ferrocene value of -4.8 eV with respect to the vacuum [17]. The PL spectra of the ruthenium compounds and PVK: PBD were measured in acetonitrile solution. The PL spectra were recorded by ocean optic spectrometer USB2000 during 405 nm irradiation. The molecular and electronic structure calculations were performed with density functional theory (DFT) using the Gaussian 03(G03) software package. The B3LYP functional [18, 19] with the LANL2DZ basis set was carried out. All geometry optimizations were performed in either C1 or C2 symmetry with subsequent frequency analysis to show that the structures are at the local minima on the potential energy surface. The electronic orbitals were visualized using Gauss View 3.0.

2. 2 Preparation of EL devices and testing. The structure of the fabricated device is as follow:

ITO/PEDOT:PSS(55nm)/PVK(60nm)/PBD(30nm)/Al(130nm) and, ITO/PEDOT:PSS(55nm)/ PVK(60nm)/PBD(30nm)/ $Ru(dpq)(COOH)_2$ complex (40nm)/Al(200nm), That is shown in Figure 1.

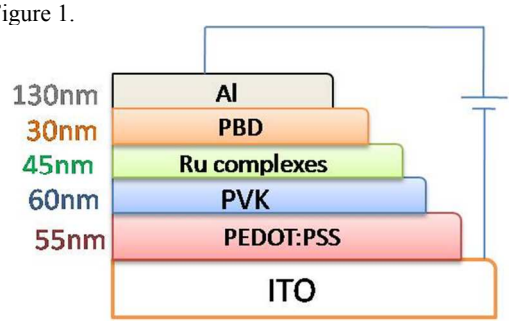

Figure 1. The layer arrangement of $Ru(dpq(COOH)_2)$-based LED.

PVK as hole-transporting and PBD as electron-transporting material were doped with ruthenium compounds. Glass substrates, coated with ITO (sheet resistance of 70 Ω/m^2), were used as the conducting anode. The ratio of ruthenium complexes for each type were 8 %Wt in PVK: PBD(100:40). PEDOT: PSS(poly(3,4-ethylenedi-oxythiophene):poly(styrenesulfonate) was used as a hole injection and transporting layer. All polymeric layers were successively deposited onto the ITO coated-glass by using spin-coating process from the solution. A metallic cathode of Al was deposited on the emissive layer at 8×10^{-5} mbar by thermal evaporation. The PEDOT: PSS was dissolved in DMF, spin coated on ITO and held in an oven at 120℃ for 2 hours after deposition. PVK, PBD and ruthenium complexes with ratio of 100: 40: 8 were blended in DMF, and then spin coated and baked at 80℃ for 1 hour. The thickness of the polymeric thin film was determined by a Dektak 8000. The EL intensity and spectra were measured with an ocean optic USB2000, under ambient conditions. In addition, a Keithley 2400 source meter was used to measure the electrical characteristics of the devices.

2. 3 Synthesis of ligands and complexes

1, 10-Phenanthroline-5, 6-dione (phendione)[20], $[Ru(phen)\ Cl_4]^-$,and $[Ru(bpy)Cl_4]^-$ [21],were synthesized by reported procedures. The syntheses of dicnq and its ruthenium (II) complexes are described below.

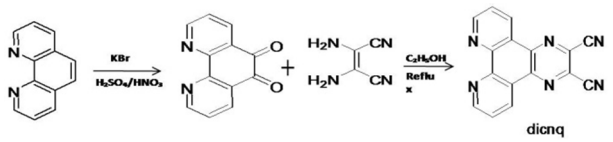

Scheme 1.Synthesis procedure of dicnq.

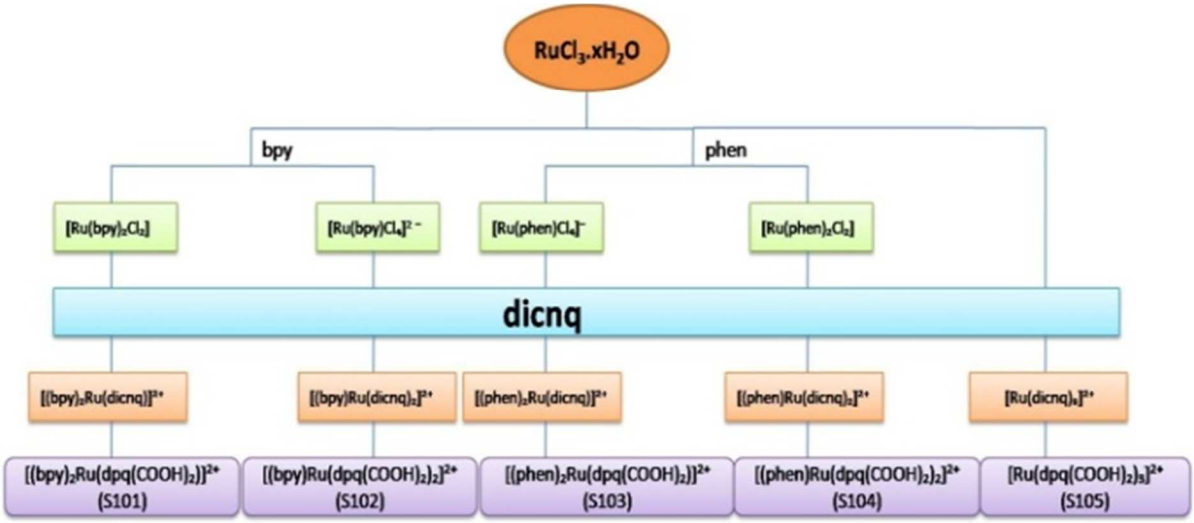

Scheme 2.Schematic representation of different synthetic approaches to S101-5.

2. 3. 1 6,7-Dicyanodipyrido[2,2-d:2',3'-f] quinoxaline (dicnq). The *dicnq* ligand was synthesized by following the reported procedures with some changes [13], phendione (210mg, 1mmol) and diaminomaleonitrile (162 mg, 1.5 mmol) were dissolved in ethanol, and the resulting solution was refluxed for 1h under a nitrogen atmosphere. The reaction mixture was cooled to room temperature, concentrated, and kept in an ice bath. Brownish-yellow needles were formed, which were filtered, washed with cold ethanol, and dried in vacuum. Yield: 80%. m. p. >250 °C. Anal. Found: C, 67.98; H, 2.19; N, 29.37. Calcd. for C16H6N6: C, 68.08; H, 2.14; N, 29.57. FAB-MS: m/z 283 (M^+).;1 H NMR (DMSO-d6, 400 MHz, TMS): 9.37 (m, 4H), 7.98 (q, 2H).

*2. 3. 2 {(bpy)₂Ru[(dpq(COOH)₂)]}$(BF_4)_2$ (S101).*A mixture of $RuCl_3$ (0.1g, 1mmol) and 2,2-bipyridine (0.16g, 2.2mmol) was dissolved in 50 ml ethanol and stirred at reflux temperature for 2h under a nitrogen atmosphere. The red precipitate, $[Ru(bpy)_2Cl_2]$, which formed was collected and washed with ethanol and ether. This product was dissolved in methanol (5ml) and added to a solution of dicnq (0.78mg, 1mmol) in hot acetonitrile (30ml), and the suspension was heated to reflux for 2 h. After cooling down to room temperature, the solution was concentrated with a rotary evaporator followed by the addition of an aqueous $NaBF_4$ saturated solution. The red precipitate was filtered and washed with cold water and ethanol. The filtrate was dissolved in 20 mL of warm 5M H_2SO_4, and the solution was deoxygenated before heating at 110-120 °C overnight. After cooling in an ice bath, the pH of this solution was increased to 4 by the addition of 5 M NaOH. An orange precipitate was formed upon addition of aqueous $NaBF_4$ and was filtered off and washed with cold water. This product was further purified by column chromatography using alumina as column support and acetonitrile/ methanol (2: 1, v/v) as the eluent. The major orange band was collected and corresponds to the desired complex. Yield: 52%.; m.p. >250 °C., Anal. Found: C, 47.110; H, 2.597; N, 1.20. Calcd. for $RuC_{36}H_{24}N_8O_4$:C, 47.102; H, 2.601; N, 1.212. ESI-MS:m/z 738. 7, [M-2BF_4], ^{1}H NMR(DMSO-d6, 400MHz): δ 9.23 (dd, 1H), 8.90(dd, 1H), 8.53(dd, 4H), 8.08(dd, 6H), 7.83-7.97(m, 4H),7.63(dd, 4H), 7.20-7.40(m, 4H).

2. 3. 3{(bpy) Ru[(dpq(COOH)₂)]₂}$(BF_4)_2$ (S102). This complex was prepared from $[Ru(bpy)Cl_4]^-$(0.17mmol) and dicnq (0.2 mmol) in a manner analogous to that employed for the synthesis of S101. The isolated solid was recrystallized from methanol-diethyl ether, after which it was future purified on an alumina column, using acetonitrile/ methanol (2: 1, v/v) as the eluent. The major orange band was collected and corresponds to the desired complex. Yield 51%., .m.p. >250 °C. Yield: 52%. m. p. >250 °C.Anal. Found: C, 47.179; H, 2.20; N, 13.180. Calcd for $RuC_{36}H_{24}N_8O_4$:C 47.187; H, 2.218; N, 13.189. ESI-MS:m/z 897.8, [M-2BF_4], ^{1}H NMR(DMSO-d6, 400MHz): δ 9.38(dd,2H), 9.18(dd,2H), 8.55(dd,2H), 8.00-8.12(m,8H), 7.81(td,1H), 7.74(dd,1H), 7.57(dd,1H), 7.29(m,2H).

2. 3. 4 {(phen)₂Ru[dpq(COOH)₂]}$(BF_4)_2$(S103). A mixture of $RuCl_3$ (0.1g, 1mmol) and 1,10-phen (0.18g, 2.1mmol) dissolved in 50 ml ethanol was stirred at reflux temperature for 2h under a nitrogen atmosphere. The red precipitate, $[Ru(phen)_2Cl_2]$, which formed was collected and washed with ethanol and ether. This product was dissolved and placed in a 100 mL round-bottom flask containing 40 mL of a methanol-water (1:1, vol/vol) mixture, and the suspension was heated to reflux for 2 h under a nitrogen atmosphere. The resulting brownish-red solution was allowed to cool to room temperature. A saturated aqueous solution of $NaBF_4$ was added to this solution to precipitate the crude complex, which was filtered off. The solid was washed with $CHCl_3$, recrystallized from acetone-ether, and vacuum-dried to obtain the pure product. Finally to achieve carboxylation, the mixture was dissolved in a H_2SO_4 solution in a manner analogous to that employed for the synthesis of S101.

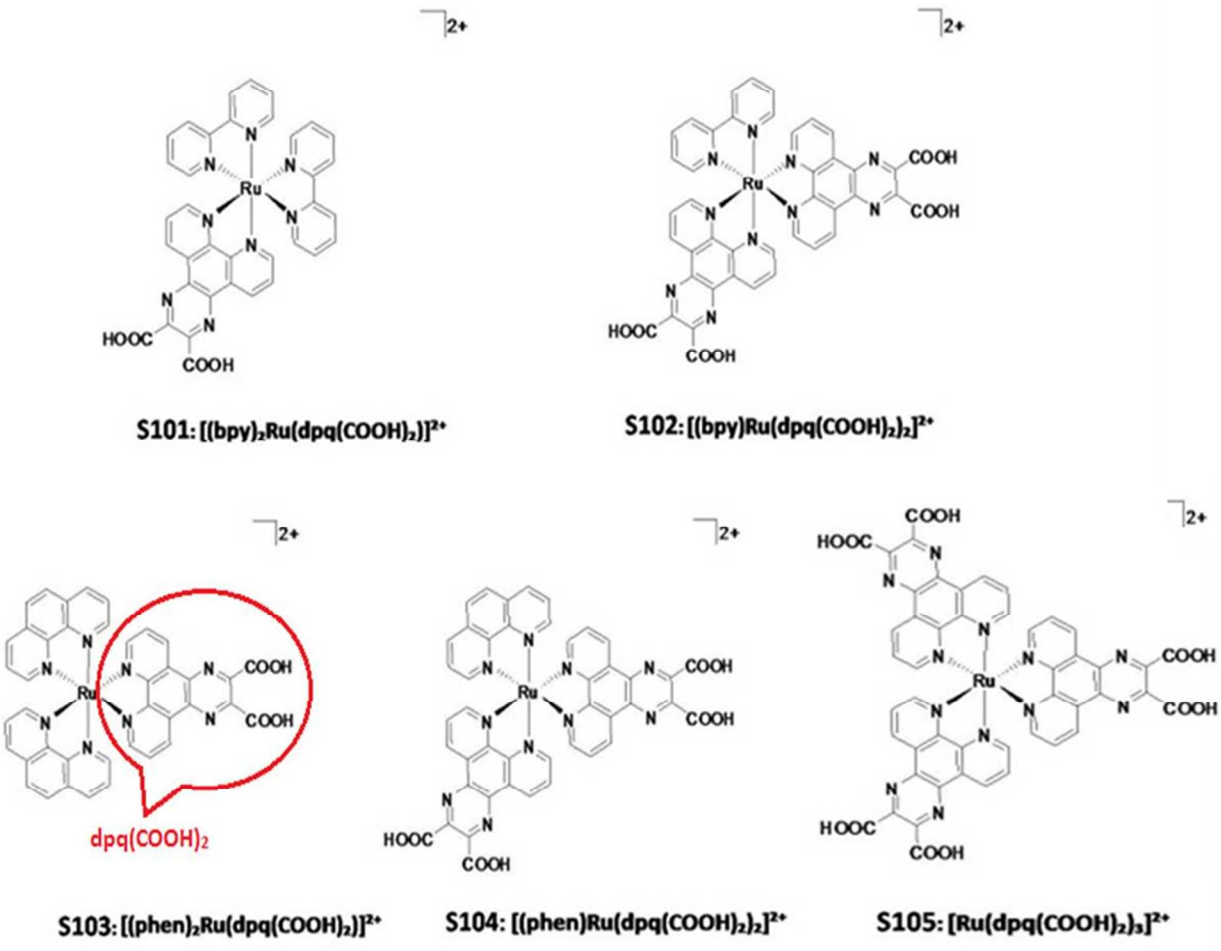

Scheme 3. Molecular structure of S101-105.

The isolated solid was recrystallized from methanol-diethyl ether, after which it was further purified on an alumina column, using acetonitrile/ methanol (2: 1, v/v) as the eluent. The major orange band was collected and corresponds to the desired complex. Yield 41%.; m.p. >250 °C.; Anal. Found: C, 50.320; H, 2.521; N, 11.598. Calcd for $RuC_{36}H_{24}N_8O_4$: C 50.312; H, 2.532; N, 11.654. ESI-MS:m/z 781.7, [M-2BF_4]. ^{1}H NMR(DMSO-d6, 400MHz): δ,9.01(dd, 4H), 8.63(s, 4H), 8.43(m, 2H), 8.21(dd, 4H), 8.11(m, 2H), 7.79(m ,4H).

2. 3. 5 {(phen) Ru[dpq(COOH)$_2$]$_2$}(BF$_4$)$_2$ (S104). This complex (S104) was prepared, using the same procedure for complex S103 except we used 1 equiv (phen) (0.15 g, 0.34 mmol) and 2 equiv dicnq(0.21g, 0.78 mmol). This product was further purified by column chromatography using alumina as the column support and acetonitrile/ methanol (2: 1, v/v) as the eluent. The major dark brown band was collected and corresponds to the desired complex. Yield: 52%.; m. p. >250 °C.; Anal. Found: C, 48.131; H, 2.151; N, 12.598. Calcd. for $RuC_{36}H_{24}N_8O_4$:C 48.125; H, 2.144; N, 12.112. ESI-MS:m/z 922.8, [M-2BF_4].;^{1}H NMR(DMSO-d6, 400MHz): δ, 10.12(dd, 4H), 9.57(dd,2H), 9.12(s,2H), 8.89(m, 2H), 8.61(dd,4H), 8.23(dd, 4H), 8.11(m, 2H).

*2. 3. 6 {Ru[dpq(COOH)$_2$]$_3$}(BF$_4$)$_2$(S105).*Hydrated ruthenium trichloride (1mmol, 0.15 g) and dicnq (0.6 g, 3.1 mmol) were refluxed in 40 mL of a methanol-water (1:1, vol/vol) mixture for 4 h. The resulting solution was allowed to cool to the room temperature and filtered. A saturated aqueous solution of $NaBF_4$ was added to the red filtrate to affect precipitation of the crude product, which was filtered off, washed with $CHCl_3$ and recrystallized from acetone-ether. Finally to achieve carboxylation the mixture was dissolved in H_2SO_4 solution in a manner analogous to that employed for the synthesis of S103. The isolated solid was recrystallized from methanol-diethyl ether, after which it was further purified on an alumina column, using acetonitrile/ methanol (2: 1, v/v) as the eluent. Yield 41%.; m.p. >250 °C.; Yield: 41%. m. p. >250 °C. Anal. Found: C, 46.331; H, 1.968; N, 13.610. Calcd for $RuC_{36}H_{24}N_8O_4$:C 46.345; H, 1.952; N, 13.654. ESI-MS:m/z 1061.1, [M-2BF_4].;^{1}H NMR(DMSO-d6, 400MHz): δ, 9.87(m, 2H), 9.23(dd, 2H), 8.38(m, 2H).

3. Results and Discussion

This part of the paper is divided into three sections. In section 3.1, we present the characterization data and optical properties of Ru(dpq)$(COOH)_2$ complexes. Section 3.2 examines the DFT and TD-DFT calculations of the optimized structure. These studies will be assisted to reveal the electronic structure and electronic transfer mechanism in the prepared LED devices. Finally, section 3.3 examines the chemically modified compound, demonstrating that EL wavelength can be tuned through ancillary ligand substitution.

3. 1 Spectral and electrochemical characterizations of complexes

As the main strategy to design ruthenium polypyridyl electroluminescent, the structure of the ligands was selected by

adopting $[Ru(bpy)_3](PF_6)_2$ as a model compound and modifying it in two ways: first, with the addition of long aliphatic chains or bulky substituent, second, with the substitution of the heteroatom framework with the more conjugated phen ligand. Here, we selected the second way to design novel ruthenium polypyridyl emitter. Absorption spectra of dicnq ligand and their ruthenium(II) complexes are shown in Figure 2 and UV-Vis results are summarized in Table 1. The absorption spectrum of the dicnq ligand shows bands in the 220-400 nm regions with the most intense band being located at 265 nm. The intense peak at 265 nm is related to 'phen' portion whereas the additional peaks of less intensity at higher wavelength (305, 347, and 365 nm) arise from the 'quinoxaline' portion of dpq [22]. In the UV-Vis spectra of the five complexes, the ultraviolet regions show intense bands arising from the intra ligand transitions (π-π^*) due to the coordinated phen, bpy, and dicnq with metal [11]. This confirms that the UV spectra of the complexes reflect an essential absorption of the ligands. Broad absorption bands in the visible region 450-600 nm were assigned to MLCT transitions from Ru(4d) orbitals to ligand-centered π^* orbitals.

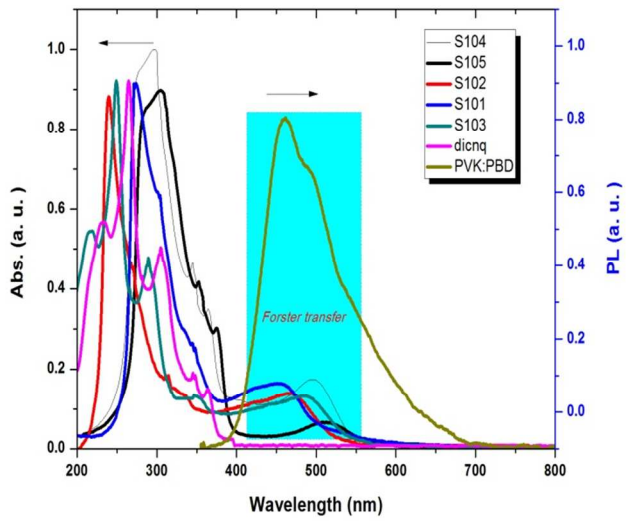

Figure 2. Absorption spectra of dicnq ligand and complexes (S101-105) and PL spectrum of PVK:PBD (λ_{exc}=405 nm) in acetonitrile solution 10^{-5} mol lit^{-1}. The inset shows the overlap between absorption spectra of complexes and PL spectrum of PVK: PBD.

It was also proposed that several transitions may be involved in the MLCT absorption bands of Ru(II) complexes, such as dp(Ru)/p*(bpy),dp(Ru)/p*(phen)dp(Ru)/p*[dpq(COOH)$_2$] [23]. Our DFT/TDDFT calculations support this assignment which will be discussed in following paragraphs.

The PL spectra of ruthenium(II)–polypyridyl complexes are largely attributed to the ^{3}MLCT and $^3\pi$-π^* states in the literature which are populated via an ultrafast ISC process from directly photoexcited ^{1}MLCT states [24]. Generally, the transition arises from the promotion of an electron from a filled t_{2g}-orbital on the metal to a vacant π^*-orbital on the neutral, aromatic bpy/phen-ligand. The ligand-centered $^3(\pi$-$\pi^*)$ transition typically involves the movement of electrons between filled and vacant π-orbitals on the bpy/phen-ligands [25]. In particular, there is a degree of mixing between these two emissive states in the ruthenium polypyridyl complexes. In all cases (S101-105), the luminescence emission clearly originates from ^{3}MLCT states involving the polypyridyl ligands, as indicated by the position and shape of the emission band which are in the expected range for Ru–polypyridyl complexes [26]. From Figure 3 and Table 1, the PL emission band shifts to higher wavelengths with λ_{max} = 598, 611, 620, 633 and 646 nm, in concert with the decreasing of HOMO-LUMO band gap due to the substitution of ancillary ligands in complexes S101-105, respectively. The emission of S105 is red-shifted in wavelength (λ_{max}= 570 nm) to S101-104 indicative of effects of the electron-withdrawing groups dicnq compared to the un-substituted bpy or phen ligands. The emission quantum yield (Φ) was calculated for each compound according to the reference available in the literature [27]. As given in Table 1, the emission quantum yields of the Ru complexes were obtained between 0.058 and 0.007. The obtained quantum yield of complexes are acceptable data among the reported quantum yields of Ru (dicnq) complexes for future PL and EL studies (more details are given in ESI S2) .

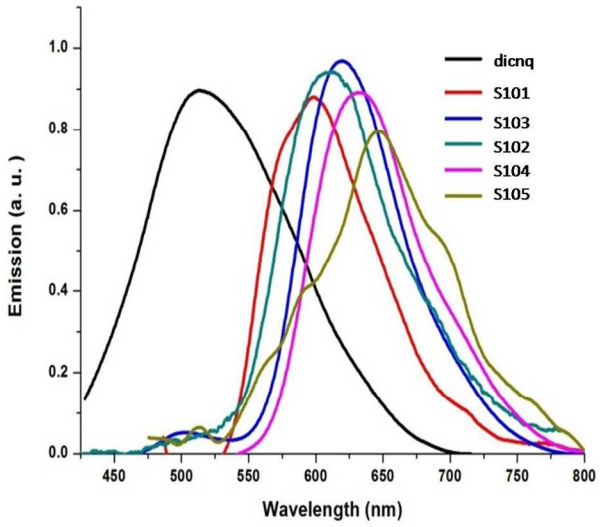

Figure 3. PL spectra of $Ru(dpq)(COOH)_2$ complexes (S101-105) and dicnq in acetonitrile solution 10^{-5}mol lit^{-1} (λ_{exc}=405 nm).

The obtained quantum yield of S101 is about 2 fold higher than that found for $Ru(phen)_3^{2+}$ as a reference sample, which shows a fluorescence efficiency of 0.025 under the same experimental conditions. The quantum yield for the protonated complex S105 with 6 carboxyl moieties (ϕ= 0.0066) is approximately half that of the corresponding S101 with 2 carboxylic acid moieties. The proton-induced quenching could be one of the accounts for the lower- quantum yield from the acidic forms of the complexes due to the deactivation of charge-transfer excited states [28]. This means that there is a limitation to incorporate of withdrawing ligands which can produce H-banding interactions. These different quantum yields indicate that the substitution profile of the ancillary ligand can impart significant influence on the photophysical properties of the $[Ru(dpq)(COOH)_2]$ complexes. The changes in the luminescence behavior of the complexes with the ancillary ligand substitution are quite interesting and somewhat difficult to unravel. To our knowledge, there has been no detailed discussion about the energy transfer mechanism for this initial step in excited-state evolution in this class of molecules. So, more photophysical studies are required to improve the understanding of the relationship between the population of ^{3}MLCT of ligands and the radiative and non-radiative process. These studies should involve femtosecond time resolved transient absorption spectroscopy. FT-IR spectra of dicnq and $Ru(dpq)(COOH)_2$ complexes are shown in Figure 4.

In the infrared spectra of the [Ru(dicnq)] complexes, the cyano

stretching frequency of dicnq was present at 2239 cm^{-1} and this band appeared at 2237 cm^{-1} in their precursor [Ru(dicnq)] complexes thus confirming that chelating of dicnq to ruthenium has not affected the quinone part of this ligand and the CN that the two cyano groups of this ligand are not involved in the metal-ligand bonding [11,22]. As shown in Figure 4, the cyano stretching frequency at about 2230 cm^{-1} has been removed which indicates the conversion of dicnq moieties to dpq$(COOH)_2$ groupsin S101-105.

Table 1.UV–vis absorption and emission properties of dicnq and Ru (dpq$(COOH)_2$) complexes measured in acetonitrile. (λ_{exc}=405 nm)

Compound	Absorbance	Photoluminescence	
	λ_{max} , nm(logϵ)	λ_{max} nm	,Φ
dicnq	263(4.36), 301(4.12), 336(3.6), 354(3.5)	513	
S101	278(4.76), 344(4.42), 366(4.3), 492(4.22)	598	0.058
S102	298(4.78),346(4.42),371(4.36), 511(4.92)	611	0.011
S103	279(4.34),343(3.8),366(3.6),504(3.7)	620	0.034
S104	274(4.56),304(4.12),356(4),448(3.8)	633	0.009
S105	274(5.02),302(4.7),356(4.3), 460(4.1)	646	0.007

In the IR spectra of the five Ru complexes, the pure compounds with carboxylic acid groups displayed characteristic bands at ca. about 1700 cm^{-1}, due to the conjugated C=O stretch in the carboxylic acid groups. The other prominent bands between 1600 and 1300 cm^{-1} are due to the many (C=C) stretching modes of polypyridyl circles [29], while the larger broad stretching band centered at 3397 cm^{-1} is due to the adsorbed moisture of the dyes [30].

The redox behavior of the complexes was investigated in acetonitrile solution by cyclic voltammetry (CV), at room temperature. It is well established that the redox processes in Ru(II) –polypyridyl complexes are mainly localized either on the metal center (oxidations) or on the ligands (reductions) [31].

In the potential range -1.8 to +1.7 V *vs.* Ag/AgCl at a scan rate 100 mV s^{-1} five redox couples are observed. The voltammograms display the Ru(III)/Ru(II) couple at positive potentials and the ligand reductions appear at negative potentials compared with Ag/AgCl. The oxidation couple at 1.32/1.4V is almost reversible in nature as is evident from the i_{pa}/i_{pc}= 0.95 and peak-to-peak separation, ΔEp = 80 mV (Fig. 5A). The redox reaction is assigned to Eq. (1)

$$[Ru(phen)_2dpq(COOH)_2]^{3+} + e^- \rightarrow [Ru(phen)_2dpq(COOH)_2]^{2+} \quad (1)$$

The effect of scan rate on this electron transfer process is given in Figure 6. As this figure illustrates, there is a linear relationship between the peak current and the square root of the scan rate ($v^{1/2}$), in the 10 to 800 mV s^{-1} range (Figure 6A). This behavior is diagnostic of an electron transfer process controlled by diffusion. This finding shows the reversibility of this redox process. A reduction wave for complex dpq in S103 occurs at $E^{o'}$ = -0.8 V (reversible in nature with the i_{pa}/i_{pc}= 0.96 and peak-to-peak separation, ΔE_p = 60 mV) (Figure 5A) [32]. The successive reduction of phen occurs at -1.2, -1.39, -1.56 V which are quasi or irreversible in nature (Figure 5B) [32, 13]. The similar pattern is also observed for other complexes (ESI, S3). The invariance of the positions of the four reductions with different ancillary ligands in this system supports the assertion that the available LUMO is dominantly of ligand π^* character. This is in agreement with the electrochemical behavior of homologue specie previously studied and the results of the quantum calculations [33].

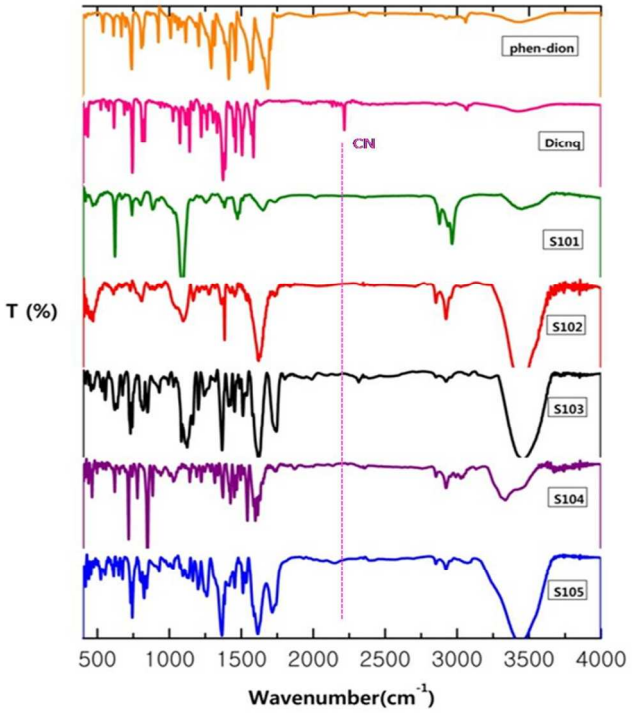

Figure.4. FT-IR spectra of phendione, Dicnq and S101-105.

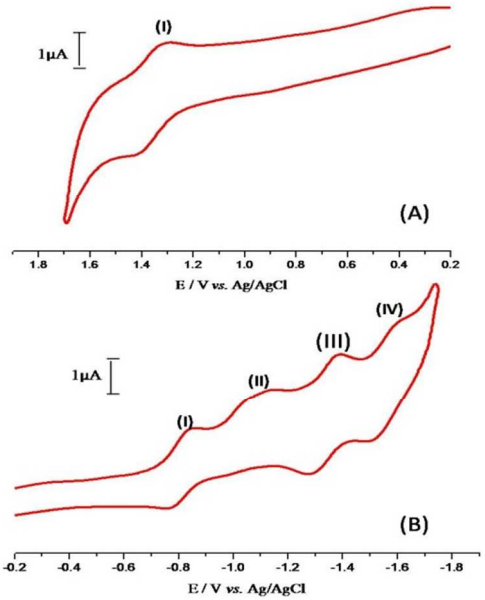

Figure 5. Cyclic voltammograms of S103 in 0.1 M TBAP/MeCN solution at a Pt disk electrode (2 mm diameter), T = 25°C, scan rate 100 mVs^{-1}: (A) Scan from -0.2 to -1.7 V; (B) scan from 0.2 to 1.7 V.

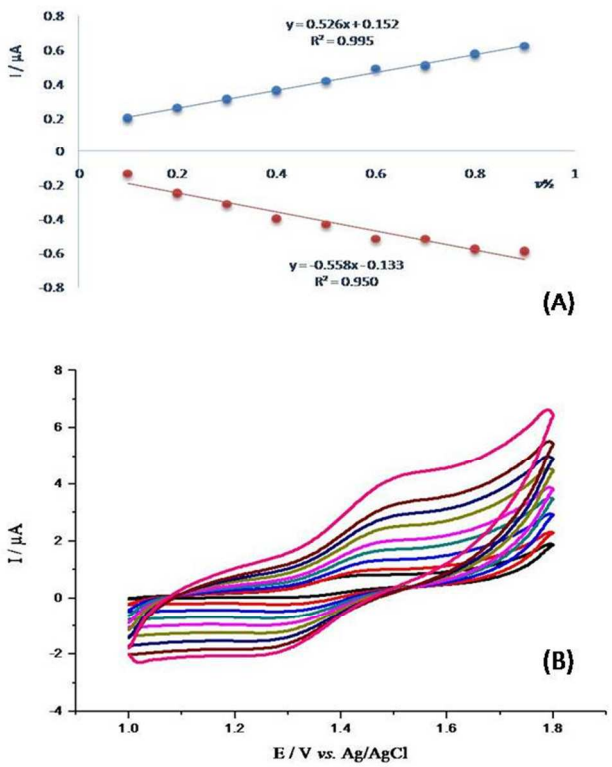

Figure 6. Effect of scan rate on the voltammograms of S103. The scan rates were maintained in the range of 10 to 800 mVs. (A) Plots of peak currents (i_P) vs. square root of scan rate (B).

3.2 DFT and TD-DFT calculation

To elucidate the electronic structure and gain further insight into the electrochemical and optical properties of S101-105, all ground-state geometry optimization calculations are performed. Time-dependent (TD- DFT) calculations were carried out on the optimized geometries. Table 2 gives the vertical excitation energies, corresponding excitation wavelengths and oscillator strengths, predominant orbitals involved in singlet-singlet transition obtained from TD-DFT calculations for S101-S105, while the selected MOs and the energy diagram are depicted in Figure 7, 8. HOMO-2 and HOMO-1 are completely localized on the Ru metal for all complexes, although some electron density of these MOs is also found on bpy ligand for S101 and S102 and phen ligand for S103 and S104. As shown in Figure 7, HOMO shows a total overlap between Ru metal and bpy ligands for S101 and S102 and also shows overlap between Ru metal and phen for S103 and S104. The LUMO orbitals are also located on one or two dpq$(COOH)_2$ moieties for S101-S104 ,while LUMO+1 and LUMO+2 orbitals show a total overlap between dpq$(COOH)_2$ and bpy ligands for S101 and S102. Thus, the LUMO+2 and LUMO+1 are ligand-based, with comparable contributions from bpy, phen and dpq$(COOH)_2$, while the LUMO is essentially dpq$(COOH)_2$ based. The HOMOs orbital of S105 are delocalized on Ru metal and the proximal part of the dpq$(COOH)_2$ ligands, while the electron density of the LUMOs are located on the distal portions of the dpq$(COOH)_2$ ligands. As an important result, the introduction of carboxylic groups decreases the band gap of Ru complexes. Thus, the S105 with three dpq$(COOH)_2$ ligands presents a HOMO–LUMO energy gap of 2.25 eV which is smaller than the band gap calculated for S101(2.51 eV), S102 (2.45), S103 (2.37), S104 (2.30). Also, the presence of the electron-withdrawing carboxylic groups stabilizes the Ru d-orbitals and leads to a change in the order of energies of the frontier occupied orbitals. Overall, the frontier orbitals of S105 are shifted to lower energies relative to those of S101-S104 which will affect the EL properties. As expected, MLCT transitions are well described by the TD-DFT approach. All these transitions are dominated by MLCT bands, corresponding to a single excitation from d orbital of the Ru and π orbital of ligands to π* orbital of the ligands. In particular, the lowest band corresponds to a HOMO/LUMO excitation, whereas the higher involves a lower d orbital and a higher empty π * orbital. The latter is a compact π* orbital localized on rings of each bpy/ phen and dpq$(COOH)_2$ ligands.

3.3 EL properties

To study the electroluminescence (EL) properties of the ruthenium complexes, LED devices were fabricated using [Ru(dpq$(COOH)_2$)] as the light emitting active layer. A blend of PVK and PBD which have balanced charge transporting ability were selected as the host [34]. The reason for choosing PVK: PBD blends, rather than PVK itself, is the better overlap of the PL of the blend with the absorption spectra of complexes (Figure 2). A better match in the donor PL and acceptor absorption would result in a better energy transfer. After the control of reaction parameters, the efficient ratio of 100:40:8 for PVK: PBD: Ru(dpq)$(COOH)_2$ was suggested, which reduces the risk of excimer formation and increases the stability of the device.

Figure 9 shows the EL corresponding results obtained for an ITO | PEDOT-PSS | [Ru(dpq$(COOH)_2$)] complex /PVK:PBD| Al device poised at 16V. An emissive layer without the ruthenium complex was fabricated to record the PVK: PBD EL spectrum and to find a relation between EL spectra of ruthenium compounds and PVK: PBD EL in order to separate it from the emission of ruthenium complexes. The emitters, S101-105, exhibit the efficient emissions with maximum emission peaks of 485, 494, 515, 533 and 572 nm, respectively, as shown in Figure 9 and summarized in Table 3, which depend on the ancillary ligand substitution. As shown in Figure 9, the wavelength of EL increases when increasing the number of substituted dpq$(COOH)_2$ ligands in S101-105 complexes.

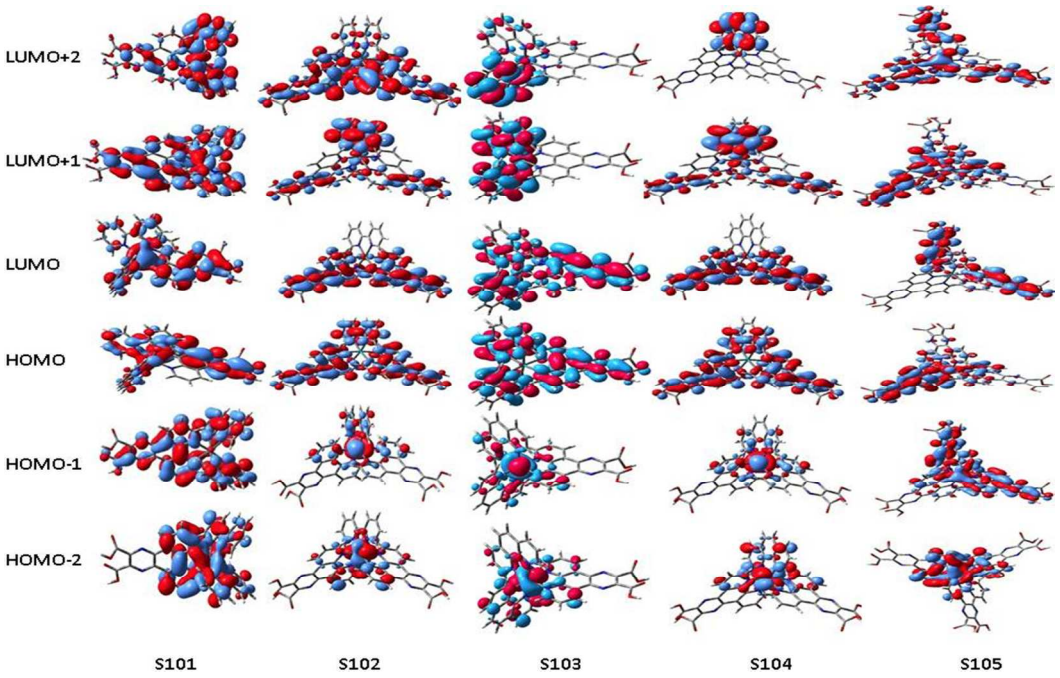

Figure. 7.Schematic representation of the molecular orbitals of S101 to S105 obtained from DFT calculation

Using both different ancillary ligands and withdraw groups gives rise to a gradual change in the LUMO–HOMO energy gap, thus allowing for the stepwise tuning of the band-gap from 2.51 for complex S101 to 2.25 eV for complex S105, as clearly shown in Figure 8. The increase in the energy gap of these ruthenium complexes should result in the blue shift of PL and EL emission. Also notable in these EL spectra is the observed blue shifted EL maxima bands compared to PL maxima bands. The EL emissions of all complexes have different maxima compared to their PL spectra which were blue-shifted by ca. 80-120 nm. Spectral shift, especially blue shift, in peak position of EL spectrum of OLED with respect to its PL counterpart has been observed. Unfortunately, the reason is not completely clear, but it seemed that this is related to the polarity and the conjugation of the whole molecules [35]. Another reason may be an interaction of the dye molecules with the embedding matrix. This leads to a shift of the emission wavelength of each dye molecule, depending on its environment [36]. In multilayer systems, the various shifts result in a spectrally broadened emission. The spectral shift could be attributed to electron-hole recombination from inter band states due to the formation of dye aggregates [37].

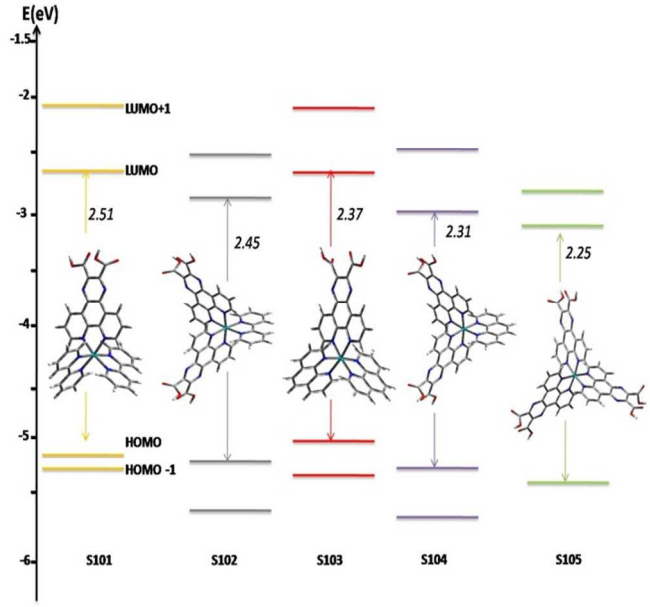

Figure 8. Diagram of the two highest occupied and two lowest unoccupied molecular orbital levels of novel Ru(dpq(COOH)$_2$) complexes (S101-105). Inset: Optimized structures of synthesized novel ruthenium complexes

Table 2.Electronic properties of S101 to S105 calculated by TD-DFT.

Emitter	ΔE (eV)	exc (nm)	*f*	Assignment (HOMO = H, LUMO = L, etc.)
S101	0.49	462	0.027	H→L+2(38%) , $d_{Ru}+\pi_{dpq(COOH)_2} \rightarrow \pi^*_{dpq(COOH)_2}$
	0.54	438	0.043	H→L+1(35%), $d_{Ru}+\pi_{dpq(COOH)_2} \rightarrow \pi^*_{bpy}$
S102	0.37	485	0.026	H→L+1(83%), $d_{Ru}+\pi_{bpy}+\pi_{dpq(COOH)_2} \rightarrow \pi^*_{bpy}$
	0.41	472	0.021	H→L+3(60%), $d_{Ru}+\pi_{bpy}+\pi_{dpq(COOH)_2} \rightarrow \pi^*_{dpq(COOH)_2}$
S103	0.33	491	0.005	H→L+2(64%), $d_{Ru}+\pi_{phen} \rightarrow \pi^*_{phen}$
	0.4	477	0.035	H→L(64%), $d_{Ru}+\pi_{phen} \rightarrow \pi^*_{dpq(COOH)_2}$
S104	0.34	498	0.028	H→L+1(87%) $d_{Ru}+\pi_{phen}+\pi_{dpq(COOH)_2} \rightarrow \pi^*_{phen}$
	0.41	482	0.02	H→L+4(60%) $d_{Ru}+\pi_{phen}+\pi_{dpq(COOH)_2} \rightarrow \pi^*_{dpq(COOH)_2}$
S105	0.31	518	0.04	H→L(90%), $d_{Ru}+\pi_{dpq(COOH)_2} \rightarrow \pi^*_{dpq(COOH)_2}$
	0.38	500	0.018	H→L+3(39%), $d_{Ru}+\pi_{dpq(COOH)_2} \rightarrow \pi^*_{dpq(COOH)_2}$

This is not the same emission peak as observed in the PL spectra of S101-105; it corresponds instead to the emission observed for the heterostructure alone, i.e., carriers recombine not in the emitter layer, but in the PVK-containing layer [38].

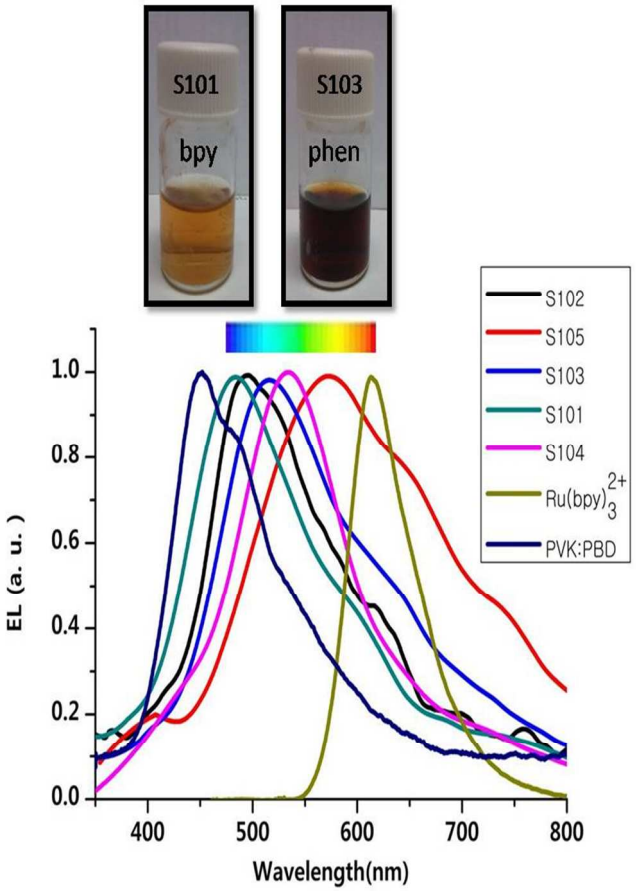

Figure 9. EL spectra of PVK: PBD and ruthenium complexes (S101-105) and $Ru(bpy)_3^{2+}$ in PVK: PBD blend. Upper: the Solution of S101 and S103.

For all complexes (S101-105), the current density rose slowly while voltage increased to 8 V and rose quickly above 10 V. The device based on (S101) reveals better characteristics than other devices (S102-105). A maximum luminance of 1357 cd/m ^{2} and a maximum emission efficiency of 2.25 cd/A at 16 V for S101 are highest among these devices. The maximum brightness obtained from S101 device is 2.5 folds higher than the best value that could be reached with S105. It is also worth mentioning that the EL efficiency decreased with the number of attached carboxyl groups. The higher efficiency EL observed for S101 doped devices are due to decreased H-aggregation than S105. The current density and luminous efficiency of S105 increases slower with the increase in applied voltage which may be attributed to aggregation of dyes due to H-bonding, increase its compatibility with the host and field-induced quenching effects [39]. A remarkable feature of LED based-S101 is its low turn-on and driving voltage, which is lower than 6.5 (V). This is among the lowest turn-on values observed in ruthenium polypyridyl single-layer OLED [40].

In particular, the luminous efficiency of complex S101 was better than that of $[Ru(phen)_3](PF_6)_2$ as a reference sample under the same conditions. The improved turn on of S101 can be attributed to using the smaller counter ion of BF_4^- instead of PF_6^- [41].

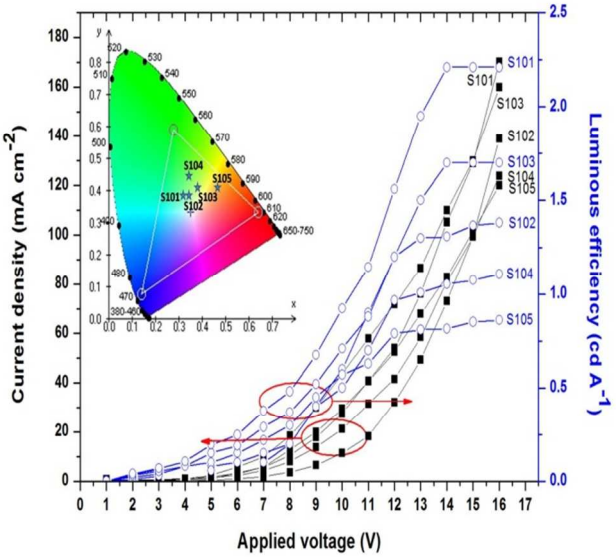

Figure 10. Current density and luminance versus applied voltage for devices (S101-105). Inset: CIE coordinates of $Ru(dpq)(COOH)_2$ emitters (S101-105).

Table 3.Device characteristics of Ru complexes (S101-105).

No.	EL_{max} [nm]	CIE [*x*, *y*]	Emission colour (CIE chromaticity diagram)	FWHM [nm]	Maximum current density, at 16[V]	Turn-on [V]	Luminous efficiency [cd A^{-1}] at [16]	Luminance [cd m^{-2}] at 16[V]
S101	485	(0.324, 0.384)	Bluish green	149.5	170.9	6.4	2.25	1357
S102	494	(0.331, 0.391)	Near white	143.7	138.9	7.2	1.38	1156
S103	515	(0.380, 0.401)	Yellow green	172.6	160.2	6.8	1.71	1233
S104	533	(0.341, 0.439)	Yellowish green	122.7	123.1	9.5	1.12	1040
S105	572	(0.465, 0.401)	Orange	219.8	118.3	7.5	0.83	850

As shown in Figure 9, S101 with two bpy as ancillary ligand has the most blue-shift in EL wavelength. In result, the EL properties of the complexes relate to the structure of ligands. So, we can control the emission properties of OLED devices by adding different ancillary ligands. We attribute this interesting phenomenon to the Forster energy transfer since there is overlap between the absorption spectra of emitters (S101-105) and emission spectrum of PVK: PBD. Such overlap between the matrix emission and dopant absorption is necessary for efficient energy transfer (one should keep in mind, though, that the absorption of the ruthenium complex in solid solution might be different) [42].

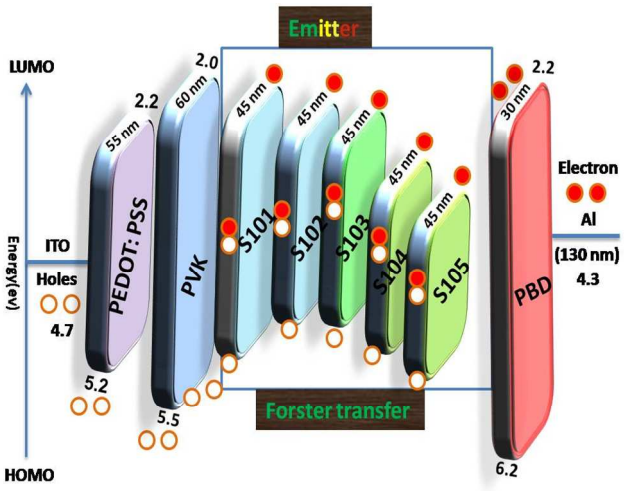

Figure 11.Schematic showing the energy levels of device and the

dynamic process of EL emission. Moreover, the arrangement of layers causing the Forster transfer of energy was resulted from the PVK: PBD host to S101-105 (Figure 9)[43]. It should be mentioned that the device structure has the potential for further optimization. For example, the use of LiF cathodes [44], and different charge transport components [45] that result in a reduction in operating voltage or increased efficiency are also applicable to this work.

Finally, we expected that the various fundamental properties elaborated in this study would be beneficial to the future development of Ru polypyridyl emitting materials for use as luminescent OLEDs.

4. Conclusion

In conclusion, we have synthesized a novel family of ruthenium dpq(COOH)$_2$ complexes and studied their electrochemical, spectroscopic and electroluminescent properties. The performance of their electroluminescent devices was dominated by ancillary ligand substitution effects. The electroluminescence emission colors ranging from orange to bluish green were obtained by tuning the ancillary ligand substitution. The two bpy ligands as ancillary ligands and one dpq(COOH)$_2$ ligand, S101, were found to be the most beneficial modifications to the arrangement of ruthenium polypyridyl complexes in terms of minimizing H-aggregation and enhancing device characteristics. The luminance and luminous efficiency of newly prepared samples were better than that of known samples [Ru(phen)$_3$](PF$_6$)$_2$. It is of interest to further study in detail the light-emitting mechanisms of the Ru(dpq(COOH)$_2$) complexes and the charge transfer states. By using different ancillary ligands and substituted groups, it is possible to prepare metal-containing π-extended ligands with different emission colors and charge transport properties. The stability and efficiency of this type of ruthenium-based light emission diodes are under investigation in our group.

Acknowledgments:

The authors wish to thank the University of Zanjan for financial supports.

References

[1] a) V. Balzani, A. Credi, M. Venturi, *Chem. Sus. Chem.* **2008**, *1*, 26; b) S. R. Dalton, S. Glazier, B. Leung, S. Win, C. Megatulski, S. J. N. Burgmayer, *J. Biol. Inorg. Chem.* **2008**, *13*, 1133; c) C. B. Spillane, N. C. Fletcher, S. M. Rountree, H. van den Berg, S. Chanduloy, , J. L. Morgan, F. R. Keene, *J. Biol. Inorg. Chem.***2007**, *12*, 797; d) X. H. Zou, B. H. Ye, H. Li, Q. L. Zhang, H. Chao, J. G. Liu, L. N. Ji, X. Y. Li, *J. Biol. Inorg. Chem.***2001**, *6*, 143; e) J. K. Barton, Science **1986**, *233*, 727; f) C. Metcalfe, J. Thomas, J. A. *Chem. Soc. Rev.***2003**, *32*, 215; g) A. E. Friedman, J. C. Chambron, J. P. Sauvage, N. J. Turro, J. K. Barton, *J. Am. Chem. Soc.* **1990**, *112*, 4960; h) R. M. Hartshorn, J. K. Barton, *J. Am. Chem. Soc.***1992**, *114*, 5919; i) K. E. Erkkila, D. T. Odom, J. K. Barton, *Chem. Rev.***1999**, *99*, 2777; j) E. Ruba, J. R. Hart, J. K. Barton, *Inorg. Chem.* **2004**, *43*, 4570.

[2] b) M. Y. Teng, Q. L. Xu, H. Y. Li, L. Wu, Y. X. Zheng, C. Lin L. Wang, *RSC Adv.***2012**, *2*, 10175; c) A. Wild, A. Winter, F. Schlutter, U. S. Schubert, *Chem. Soc. Rev.***2011**, *40*, 1459; d) V. W. W. Yam, K. M. C. Wong, *Chem. Commun.***2011**, *47*, 11579; e) G. Accorsi, A. Listorti, K. Yoosaf, N. Armaroli, *Chem. Soc. Rev.***2009**, *38*, 1690; f) P. I. P. Eliiott, *Annul. Rep. Prog. Chem., Sect. A: Inorg. Chem.***2012**, *108*, 389.

[3] a) J. Bossert, C. Daniel, *Coord. Chem. Rev.* **2008**, *254*, 2493; b) N.-Y. Chen, Y. Fan, J. Ni, *Dalton Trans.***2008**, 573; c) V. Balzani, A. Credi, M. venture, *Molecular Device and Mechanic, Concept and Perspective for the Nanoworld*, Wiley-VCH, Weinheim, Germany, 2nd edn, **2008**.

[4] a) H. Rudmann, M. F. Rubner, *J. Appl. Phys.***2001**, *90*, 4338; b) H. Rudmann, S. Shimada, M. F. Rubner, *J. Am. Chem.*

*Soc.***2002**, *124*, 4918.
[5] a) S. M. Zakeeruddin, Md. K. Nazeeruddin, R. Humphry-Baker, M. Gratzel, *Inorg. Chem.***1998**, *37*, 5251; b) J. Bolger, A. Gourdon, E. Ishow, J. P. Launay, *Inorg. Chem.* **1996**, *35*, 2937; c) V. Balzani, F. Barigelletti, P. Belser, S. Bernhard, L. De Cola, L. Flamigni, *J. Phys. Chem.* **1996**, *100*, 16786; d) A. Gourdon, J. P. Launay, *Inorg. Chem.* **1998**, *37*, 5336; e) T. Kajita, R. M. Leasure, M. Devenney, D. Friesen, T. Meyer, *J. Inorg.Chem.***1998**, *37*, 4782; f) C. Moucheron, A. K. D. Mesmaeker, S. Choua, *Inorg.Chem.* **1997**, *36*, 584; g) M. T. Indelli, C. A. Bignozzi, F. Scandola, J.-P. Collin, *Inorg. Chem.***1998**, *37*, 6084; h) R. M. Hartshorn, J. K. Barton, *J. Am. Chem. Soc.* **1992**, *114*, 5919.
[6] H. J. Bolink, L. Cappelli, E. Coronado, P. Gavina, *Inorg.Chem.* **2005**, *44*, 5966.
[7] N. E. Tokel-Takvoryan, R. E. Hemingway, A. J. Bard, *J. Am. Chem. Soc.***1973**, *95*, 6582.
[8] J. Ouyang, A. J. Bull. Bard, *Chem. Soc. Jpn.***1988**, *61*, 17.
[9] F. Kanoufi, A. J. Bard, *J. Phys. Chem.***1999**, *103*, 10469.
[10] S. Xun, J. Zhang, X. Li, D. Ma, Z. Y. Wang, *Synth. Met.***2008**, *158*, 484.
[11] B. Gholamkhass, K. Koike, N. Negishi, H. Hori, K. Takeuchi, *Inorg. Chem.* **2001**, *40*, 756.
[12] A. G. Zhang, Y. Z. Zhang, Z. M. Duan, K. Z. Wang, H. B. Wei, Z. Q. Bian, C. H. Huang, *Inorg. Chem.***2011**, *50*, 6425.
[13] A. Ambroise, B. G. Maiya, *Inorg. Chem.***2000**, *39*, 4264.
[14] K. A. O'Donoghue, J. M. Kelly, P. E. Kruger, *Dalton Trans.***2004**, 13.
[15] a) H. Shahroosvand, P. Abbasi, A. Faghih, E. Mohajerani, M. Janghouri, M. Mahmoudi, *RSC Adv.***2014**, *4*, 1150; b) H. Shahroosvand, F. Nasouti, A. Sousaraei, E. Mohajerani, A. Khabbazi, *Phys. Chem. Chem. Phys*. **2013**, *15*, 9899; c) H. Shahroosvand, F.Nasouti, E. Mohajerani, A, Khabazi, *Opt. Mater*. **2012**, *35*, 79; d) H. Shahroosvand, F. Nasouti, E. Mohajerani, A. Khabbazi, *J. Lumin*.**2013**, 135, 339.
[16] a) H. Shahroosvand, L. Najafi, E. Mohajerani, A. Khabbazi, M. Nasrollahzadeh, *J. Mater. Chem. C*. **2013**, *1*, 1337; b), H. Shahroosvand, L. Najafi, E. Mohajerani, M. Janghouri, M. Nasrollahzadeh, *RSC Adv*. **2013,** *3*, 6323**;** c) H. Shahroosvand, L. Najafi, E. Mohajerani, A. Khabbazi, M. Mhmoudi*J. Mater.Chem. C*. **2013**, *1*, 6970.
[17] (a) M. Thelakkat, H. Schmidt, *Adv. Mater*., 1998,**10**, 219. (b) S. Ashraf, M. Shahid, E. Klemm, M. Al-Ibrahim, S. Sensfuss, ,Macrol. *Rapid. Commun*.,**2006**, *27*, 1454.
[18] S. Fantacci, F. De Angelis, A. Selloni, J. Am. Chem. Soc. **2003**, *125*, 4381.
[19] Fantacci, S.; De Angelis, F.; Sgamellotti, A.; Re, N. Chem. Phys. Lett. **2004**, *396*, 43.
[20]M.Yamada, Y. Tanaka, Y. Yoshimoto, S. Kuroda, I. Shimao, *Bull.Chem. Soc. Jpn.* **1992**, *65*, 1006.
[21]R.A. Krause, *Inorg. Chim.Acta.,***1977***, 22,* 209.
[22] a) D. P. Rillema, D. G. Taghdiri, D. S. Jones, C. D. Keller, L. A. Worl, T. J. Meyer, H. A. Levy, *Inorg. Chem.* **1987**, *26*, 578; b) S. Bodige, A. S. Torres, D. J. Maloney, D. Tate, G. R. Kinsel, J. K. Walker, F. M. MacDonnell, *J. Am. Chem. Soc*. **1997**, *119*, 10364.
[23] S. Delaney, M. Pascaly, P. K. Bhattacharya, K. Han, J. K. Barton, *Inorg.Chem.***2002**, *41*, 1966.
[24]N. H. Damrauer, G. Cerullo, A. Yeh, T. R. Boussie, C. V. Shank. J. K. McCusker, *Science*, **1997**, *275*, 54; b) A. C. Bhasikuttan, M. Suzuki, S. Nakashima. T. Okada, *J. Am. Chem. Soc.,***2002**, *124*, 8398; c) J. N. Demas .D. G. Taylor, *Inorg. Chem*. **1979**, *18*, 3177, d) J. N. Demas. A. W. Adamson, *J. Am. Chem. Soc.***1971**, *93*, 1800.
[25] M. G. Colombo, H. U. Gudel, *Inorg. Chem.* **1993**, *32***,** 3081.
[26] A. Juris, V. Balzani, F. Barigelletti, S. Campagna, P. Belser. A. Von Zelewsky, *Coord. Chem. Rev*. **1988**, *84*, 85 b) ; K. Kalyanasundaram, Photochemistry of Polypyridyl and Porphyrin Complexes, Academic Press, London, 1992.
[27] C. A. Parker, Measurement of Fluorescence Efficiency; Elsevier Publishing Co.: New York, 1968; pp 261-269.
[28] (a)Md. K. Nazeeruddin, P. Pechy, T. Renouard, S. M. Zakeeruddin, R. Humphry-Baker, P. Comte, P. Liska, L. Cevey, E. Costa,V. Shklover,L. Spiccia, G. B. Deacon, C. A. Bignozzi, M. Gra1tzel, *J. Am. Chem. Soc*. **2001**, *123*, 1613. (b)N. P. Ayala, C. M. Flynn, L. Jr. Sacksteder, J. N. Demas, B. A. DeGraff, *J. Am. Chem. Soc*.**1990**, *112*, 3837. (c) C. R. Hecker, A. K. Gushurst, I.D. R. McMillin, *Inorg. Chem*.**1991**, *30*, 538.(d) K. Kalyanasundaram, Md. K. Nazeeruddin, *Inorg.Chem*. **1990**,*29*, 1888.
[29]G. C. Vougioukalakis, T. Stergiopoulos, G. Kantonis, A. G. Kontos, K. Papadopou-los, A. Stublla, P. G. Potvin, P. Falaras, *J. Photochem. Photobiol., A: Chemistry*. **2010,** *214,* 22.
[30] M. Chandrasekharam, G. Rajkumar, C. S. Rao, T. Suresh, M. Reddy, P. Reddy, Y. Soujanya, B. Takeru, Y. Jun-Ho, M. K. Nazeeruddin, M. Graetzel, *Synthetic Metals***2011,***161,* 1098.
[31] F. R. Keene, D.J. Salmon, T. J. Meyer*, J. Am. Chem. Soc*. **1977**, *99*, 2384. (b) G. A. Lawrance ,*Polyhedron*, **1985**, *4*, 817.
[32] A. Francois, R. Díaz, A. Ramírez, B. Loeb, M. Barrera, I. Crivelli, *Polyhedron***2013**, *52*, 62.
[33] C. H. Braunstein, A. D. Baker, T. C. Strekas, H. D. Gafney, *Inorg. Chem*., **1984**, *23*, 854., b) A. W. Wallace, W. R. Murphy, J. D. Petersen, *Inorg. Chim.Acta.***1989**, *166*, 41. c) Y. Sun, S. N. Collins,L. E. Joyce, C. Turro, *Inorg. Chem*. **2010**, *49*, 4257., d) Y. Sun, Daniel A. Lutterman, C. Turro, *Inorg. Chem.***2008**, *47*, 6427.
[34] Z. Yingying, S. Fangzhong, L. Meirong, Z. Ming, M. Yuguang.*Semi.Sci. Tech.***2008**, *23*, 52001.
[35] M. Li, J. Liu, C. Zhao L. Sun, *J. Organomet. Chem.***2006**, *691*, 4189.
[36] D. Avnir, V. R. Kaufman, R. Reisfeld, *J. Non-Cryst. Solids* **1985**, *74*, 395.
[37] a) C. Burgdorff, H.-G. Löhmannsröben, R. Reisfeld, *Chem. Phys. Lett.***1992**, *197*, 358; b) El-Z. M. Ebeid, S. A. El-Daly, H. Langhals, *J. Phys. Chem*. **1988**, *92*, 4565. c) M. Schneider, J. Hagen, D. Harer, K. Müllen, *Adv. Mater*. **2000**, *12*, 351.
[38] T. J. Boyd, Y. Geerts, J. K. Lee, D. E. Fogg, G. G. Lavoie, R. R. Schrock, M. F. Rubner, *Macromolecules* **1997**, *30*,3553.
[39] H. Xia, Y. Zhu, D. Lu, M. Li, C. Zhang, B. Yang, *J. Phys. Chem. B.***2006**, *110*, 18718.
[40] a) H. Xia, C. Zhang, X. Liu, S. Qiu, P. Lu, F. Shen, *J. Phys. Chem. B.***2004**, *108*, 3185; b) J. Yang, K. C. Gordon. *Chem. Phys. Lett.***2004**, *385*, 481;
[41] a) M. Buda, G. Kalyuzhny, A. J. Brad, *J. Am. Chem. Soc.***2002**, *124*, 6090
[42] A. R. Hosseini, Ch. Y. Koh, J. D. Slinker, S. Flores-Torre, H. D. Abrun, G. G. Malliaras, *Chem. Mater.***2005**, *17*, 6114.
[43] a) I. Oner , C. Sahin , C. Varlikli, *Dye. Pig.***2012**, 95, 23; b) C.C. Yap, M. Yahaya, M. M. Salleh.*Curr.Appl. Phys.***2009**, *9*, 1038.
[44] G. E. Jabbour, Y. Kawabe, S. E. Shaheen, J. F. Wang, M. M. Morrell, B. Kippelen and N. Peyghambarian, *Appl. Phys. Lett*., **1997**, *71*, 1762.
[45] M. A. Baldo, S. Lamansky, P. E. Burrows, M. E. Thompson, S. R. Forrest, *Appl. Phys. Lett.*, **1999**, *75*, 4.

Graphical Abstract: